VIP Reaction Intermediates Very Important Paper

Deutsche Ausgabe: DOI: 10.1002/ange.201502731
Internationale Ausgabe: DOI: 10.1002/anie.201502731

Time-Resolved Crystallography of the Reaction Intermediate of Nitrile Hydratase: Revealing a Role for the Cysteinesulfenic Acid Ligand as a Catalytic Nucleophile

*Yasuaki Yamanaka, Yuki Kato, Koichi Hashimoto, Keisuke Iida, Kazuo Nagasawa, Hiroshi Nakayama, Naoshi Dohmae, Keiichi Noguchi, Takumi Noguchi, Masafumi Yohda, and Masafumi Odaka**

Abstract: *The reaction mechanism of nitrile hydratase (NHase) was investigated using time-resolved crystallography of the mutant NHase, in which βArg56, strictly conserved and hydrogen bonded to the two post-translationally oxidized cysteine ligands, was replaced by lysine, and pivalonitrile was the substrate. The crystal structures of the reaction intermediates were determined at high resolution (1.2–1.3 Å). In combination with FTIR analyses of NHase following hydration in $H_2{}^{18}O$, we propose that the metal-coordinated substrate is nucleophilically attacked by the O(SO^-) atom of αCys114-SO^-, followed by nucleophilic attack of the S(SO^-) atom by a βArg56-activated water molecule to release the product amide and regenerate αCys114-SO^-.*

Nitrile hydratases (NHases, E.C. 4.2.1.84) catalyze the hydration of nitriles to the corresponding amides[1] and are the most successful industrially applied microbial catalysts.[2] NHases have been used for the production of acrylamide (greater than 95 kilotons per year worldwide), nicotinamide, and 5-cyanovaleramide and may impact the bioremediation of organic nitrile pollution.[3] NHases are composed of α- and β-subunits. In the α-subunit, the catalytic center contains a singular non-heme Fe^{3+} or non-corrin Co^{3+}, which is coordinated by two deprotonated backbone amides, two oxidized cysteines (cysteine-sulfinic acid (Cys-SO_2H), and cysteinesulfenic acid (Cys-SOH)), one cysteine thiol, and a water molecule.[4] Although Cys-SO_2H and/or Cys-SOH modifications are found in a variety of proteins, such as peroxiredoxins,[5] hydrogenases,[6] and NADH peroxidases,[7] and play diverse roles in biological systems,[8] NHase is the first protein that has shown to possess both modified cysteine residues as the metal ligands.[4a,b] FTIR analyses[9] and a combination of EPR, MCD, and low-temperature absorption spectroscopy with DFT calculations have indicated that both Cys-SO_2H and Cys-SOH are deprotonated.[10] This unique coordination geometry is common among NHase family proteins, including the Fe-type[4a] and Co-type[4b] NHases and thiocyanate hydrolase (SCNase).[11] Fe-type NHases[12] and SCNase[13] lose their catalytic activities upon alteration of the oxidation states of Cys-SO_2^- and Cys-SO^-.

Based on the crystal structures, three distinct reaction mechanisms had been proposed.[4c,d,14] Two mechanisms involve direct or indirect attack of the active water ligand whereas the other involves a substrate-coordinated intermediate. Studies on many model complexes mimicking the NHase catalytic center,[4c,d,15] and on the pH and temperature dependence of the kinetic parameters[16] have suggested the mechanism that substrate coordination to the metal is followed by nucleophilic attack of a water molecule activated by an unidentified base. Previously, we investigated the reaction mechanism of an Fe-type NHase from *Rhodococcus erythropolis* N771 (*Re*NHase) using time-resolved X-ray crystallography and a *tert*-butylisonitrile (*t*BuNC) substrate analogue, and proposed that the O atom of Cys-SO^- functions as a nucleophile to activate a water molecule that attacks the substrate coordinated to the Fe^{3+} atom.[17] However, it is unknown whether this proposed mechanism accurately reflects the catalytic mechanism for a nitrile. Recently, the substrate coordination was demonstrated using single-turnover stopped-flow spectroscopy.[18] The crystal structure of the Co-type NHase from *Pseudonocardia thermophila* JCM3095 (*Pt*NHase) in complex with boronic acids (R-BOOHs)[19] suggests that the SO^- group functions as a nucleophile to attack the coordinated nitrile carbon to form a cyclic intermediate. Following this observation, Hopmann presented a unique mechanism involving disulfide bond formation between the Cys-SO^- and the cysteine thiol ligands.[20] However, this mechanism remains uncertain because R–BOOHs have been previously shown to act as general trapping agents for sulfenic acids to form similar adducts

[*] Dr. Y. Yamanaka, Dr. K. Hashimoto, Dr. K. Iida, Prof. K. Nagasawa, Prof. M. Yohda, Prof. M. Odaka
Department of Biotechnology and Life Science
Graduate School of Technology, Tokyo University of Agriculture and Technology, Koganei, Tokyo 184-8588 (Japan)
Prof. M. Odaka
Department of Life Science
Faculty and Graduate School of Engineering and Resource Science
Akita University, Akita City, Akita 010-8502 (Japan)
E-mail: modaka@gipc.akita-u.ac.jp
Prof. K. Noguchi
Instrumentation Analysis Center
Tokyo University of Agriculture and Technology
Koganei, Tokyo 184-8588 (Japan)
Dr. Y. Kato, Prof. T. Noguchi
Division of Material Science, Graduate School of Science
Nagoya University, Furo-cho, Chikusa-ku, Nagoya 464-8602 (Japan)
Dr. H. Nakayama, Dr. N. Dohmae
Global Research Cluster Collaboration Promotion Unit, RIKEN
2-1, Hirosawa, Wako-shi, Saitama 351-0198 (Japan)

Supporting information for this article is available on the WWW under http://dx.doi.org/10.1002/anie.201502731.

(R–B–O–S–R′) with sulfenic acids in aqueous media.[21] Moreover, structural evidence for disulfide bond formation is lacking.

In the present study to elucidate the catalytic mechanism, we monitored the hydration of pivalonitrile (PivCN) in crystals of the mutant *Re*NHase, βR56K, using time-resolved X-ray crystallography. βArg56 is conserved among all known NHase family proteins and is the only residue that forms hydrogen bonds with both oxidized cysteines.[4a,b,11] The k_{cat} and K_m value of βR56K are 4.6×10^2 times smaller and approximately three times larger than those of the wild-type, respectively.[22] Herein, we present the first crystal structures of the reaction intermediates of NHase at high resolution (1.2/−1.3 Å; see the Supporting Information, Table S1). Together with the results of FTIR analyses using ^{18}O-labeled water, we propose the first catalytic mechanism of NHase based on solid structural evidence.

*Re*NHase is inactivated by the nitrosylation of the Fe^{3+} ion in the dark but immediately re-activated by photoinduced denitrosylation.[23] Because nitrosylated *Re*NHase is extremely stable, all crystals were prepared in their nitrosylated form in the dark. Crystals of nitrosylated βR56K were soaked with PivCN in the dark. The structure of nitrosylated βR56K in complex with PivCN (PDB code: 3WVE) is essentially identical to that of wild-type *Re*NHase in complex with *t*BuNC (PDB code: 2ZPE),[17] except for the mutated site (Figure 1). An NO molecule is observed 2.0 Å from the Fe^{3+} atom, as observed in the structure of the nitrosylated

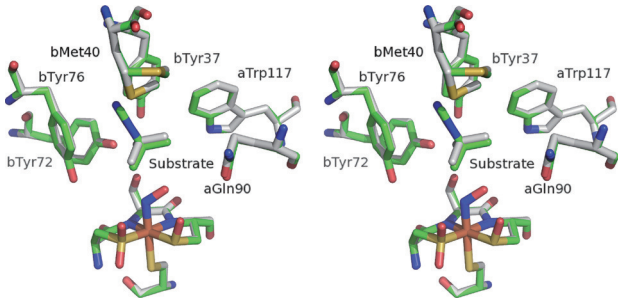

Figure 1. Stereoview of the superposed structures of the region surrounding the catalytic center of wild-type *Re*NHase in complex with *t*BuNC (PDB ID: 2ZPE) and the βR56K mutant in complex with PivCN (PDB code: 3WVE). Both enzymes are in the nitrosylated state. C (βR56K) green, C (wild-type) gray, N blue, O red, S yellow, Fe orange. In both *Re*NHases, the Sγ of βM40 adopts two conformations (lower and upper) with occupancies of lower/upper = 0.4:0.6. The movement of βM40 to the upper conformation has been suggested to result from the binding of a substrate (analogue) to the substrate binding site.[14] a and b in the amino acid residues labels indicates α and β subunits.

wild-type in complex with *t*BuNC.[17] A PivCN molecule exhibits a direction that is highly similar to that of the *t*BuNC molecule in the wild-type-*t*BuNC complex, despite a position that is 0.2 Å above that of *t*BuNC. As observed in the wild-type-*t*BuNC complex, βMet40 adopts two conformations owing to steric hindrance of the substrate. The hydrogen bonding network surrounding the catalytic center is also highly similar to that of wild-type *Re*NHase, even in the presence of the respective substrates (Supporting Information, Figure S1).

The catalytic reaction was initiated using light illumination at 293 K and proceeded for up to 700 min. Throughout the experiments, the overall structures remained nearly unaltered, except for the region above the Fe^{3+} center. Snapshots of the region surrounding the catalytic center at 0, 5, 25, 50, 120, and 700 min are shown in Figure 2. The omit

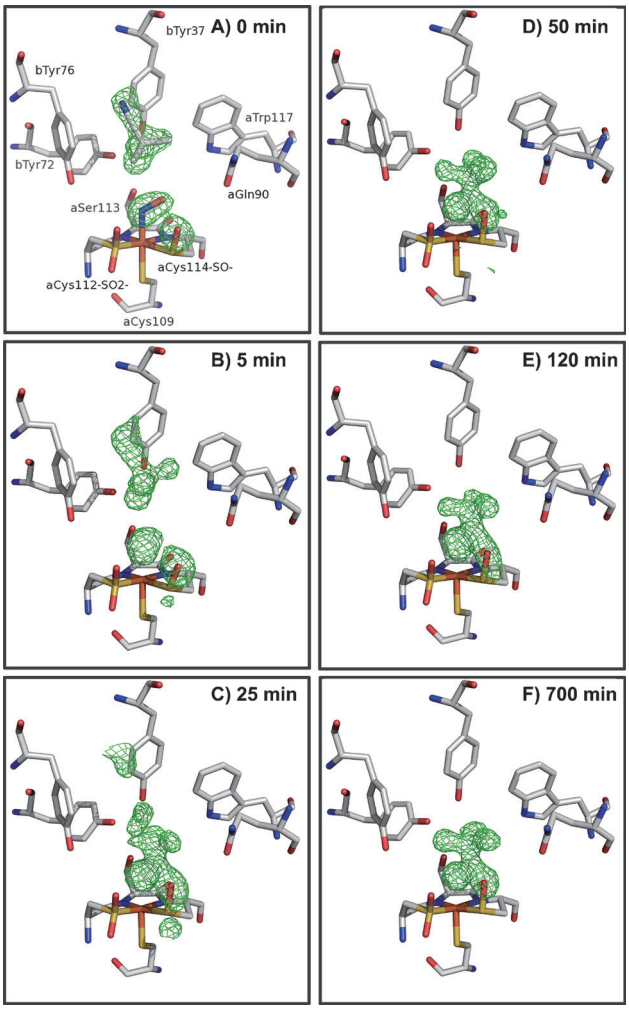

Figure 2. Time-resolved structures of the region surrounding the non-heme Fe^{3+} center of the βR56K mutant *Re*NHase. Omit maps around the catalytic center (contoured at 3.0 σ in green) are superimposed on the refined structures. *Re*NHase in complex with PivCN following light illumination for A) 0, B) 5, C) 25, D) 50, E) 120, and F) 700 min. The NO, substrate and the O atom of αCys114-SO^- were excluded from the calculations. C gray, N blue, O red, S yellow, Fe orange. a and b in the amino acid residues labels indicates α and β subunits. PDB codes for the structures of the βR56 K mutant *Re*NHase in complex with PivCN following illumination for 0, 5, 25, 50, 120, or 700 min are 3WVE, 3X26, 3X20, 3WVD, 3X24, and 3X25, respectively.

map was superimposed in each structure. Before illumination (0 min), electron densities corresponding the NO molecule and the O atom of αCys114-SO^- were observed at the sixth ligand site and the above of the S atom of αCys114, respectively. Furthermore, electron density for PivCN is

observed in the pocket close to the side chain of βTyr37 (Figure 2A). At 5 min (Figure 2B), the electron density at the sixth ligand site was slightly attenuated, reflecting the initiation of the release of the NO molecule. At 25 min (Figure 2C), the electron density of the substrate at the original position is attenuated, and in turn, a new electron density coordinated to the Fe^{3+} atom was observed. Considering the loss of the electron density at the initial substrate position, the new electron density should be that of the substrate coordinating to the Fe^{3+} atom. Nearly all of the electron density derived from the substrate is coordinated to the Fe^{3+} atom at 50 min (Figure 2D). At 120 min, the omit electron density map is similar to that at 50 min (Figure 2E). We examined 32 snapshots from 120 min to 700 min (The detailed time points examined are given in the Experimental Section in the Supplementary Information). However, the omit map coordinated to the Fe^{3+} atom was not altered (Figure 2F). These results unambiguously confirm substrate coordination to the Fe^{3+} atom during catalysis. The angle between the C atom of the pivaloyl group and the C and N atoms of the CN group is no longer linear; rather, these three atoms and the sulfenyl oxygen atom of αCys114-SO^- lie in a single plane. To identify the electron density coordinated to the Fe^{3+} atom at 50 min, PivCN or the pivalamide (Piv-$CONH_2$) product was included in the calculations, and the omit map was superimposed on the refined structures. The refined model of PivCN was distorted unrealistically and did not fit the observed electron densities in the omit map (Figure 3A), whereas Piv$CONH_2$ fits the density well (Figure 3B). However, the O_{amide}(Piv$CONH_2$)–O(αCys114-SO^-) distance is too close (0.7 Å; Figure 3B), and negative electron density corresponding to one O atom was observed around the O_{amide}(Piv$CONH_2$) and O(αCys114-SO^-) atoms (Supporting Information, Figure S2B). These results indicate that when the Piv$CONH_2$ product was positioned as shown in the omit map, the S–O bond in the SO^- group should be broken. In contrast, when the O(αCys114-SO^-) atom was excluded from the calculation, the negative electron density around the O_{amide}(Piv$CONH_2$) atom dramatically decreased (Supporting Information, Figure S2C). Thus, the results clearly demonstrate that this time point reflects the transient state structure immediately following the hydration reaction, and that the nitrile N atom that is coordinated to the Fe^{3+} atom is nucleophilically attacked by the O atom of αCys114-SO^- to form a cyclic imidate intermediate. The formation of cyclic intermediate species is consistent with the mechanism proposed based on the structures of the Co-type *Pt*NHase in complex with R-BOOHs.[19]

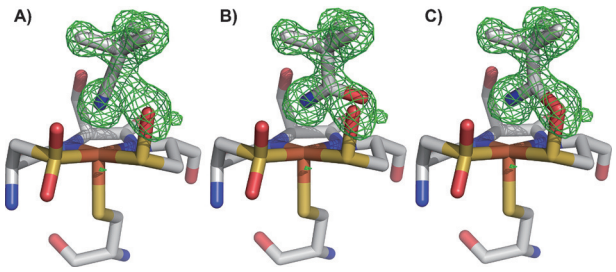

Figure 3. Structure surrounding the non-heme Fe^{3+} center of the βR56K mutant *Re*NHase in complex with PivCN following light illumination for 50 min. Omit map around the catalytic center at 50 min (contoured at +3.0 σ in green) is superimposed on the refined structure. A) The PivCN substrate was included in the calculation; B) the Piv$CONH_2$ product was included in the calculation; and C) the Piv$CONH_2$ product was included but the sulfenyl oxygen of αCys114-SO^- was excluded in the calculation. C gray, N blue, O red, S yellow, Fe orange.

Following the generation of the cyclic reaction intermediate, a water molecule activated by a base attacks the S atom of αCys114-SO^- or the C atom of the CN group to produce the amide product and regenerate the SO^- group. The water O atom is trapped in αCys114-SO^- in the former mechanism, whereas it becomes the amide O atom of the product in the latter mechanism. To investigate this step in catalysis further, we performed the nitrile hydration in $H_2{}^{18}O$ using wild-type *Re*NHase, followed by FTIR analyses. Figure 4A (blue line) shows a light-induced FTIR difference spectrum of *Re*NHase incubated in $H_2{}^{18}O$ prior to the hydration reaction, representing the structural changes of *Re*NHase upon photoreactivation.[9,23,24] Prominent bands at (1156–1149)/1126 and (1040–

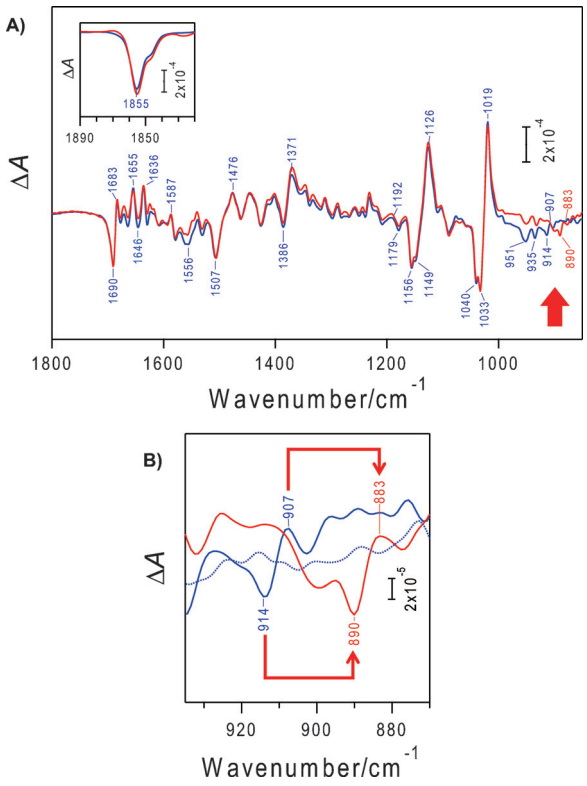

Figure 4. Light-induced FTIR difference spectra of NHase in $H_2{}^{18}O$ without treatment (blue line) and following the hydration reaction with methacrylnitrile in $H_2{}^{18}O$ and subsequent NO addition (red line). a) The 1800–850 cm^{-1} region. The inset shows an NO stretching band at 1855 cm^{-1} indicative of the release of NO from the non-heme iron center upon photoactivation. The red arrow indicates the region in which the spectral change is observed. b) An expanded view (935–870 cm^{-1}) of the SO stretching region of Cys-SO^-. The dotted blue line represents a dark-minus-dark spectrum of *Re*NHase without treatment, corresponding to the noise level.

1033)/1019 cm^{-1} and a minor signal at 914/907 cm^{-1} are virtually identical to the asymmetric and symmetric SO_2 stretching vibrations of αCys112-SO_2^- and the SO stretch of αCys114-SO^-, respectively, which have been previously assigned for *Re*NHase prepared in $H_2{}^{16}O$,[9] indicating that the oxygen atoms of the αCys-SO_2^- and αCys-SO^- groups were not exchanged with ^{18}O during incubation in $H_2{}^{18}O$. The FTIR difference spectrum of *Re*NHase, which was reacted once with methacrylonitrile in $H_2{}^{18}O$ and then nitrosylated again (Figure 4 A, red line) is also highly similar to that of *Re*NHase in $H_2{}^{18}O$ without catalysis (Figure 4 A, blue line). In fact, the spectral features and peak frequencies are identical in the 1890–920 cm^{-1} region. However, a clear difference was observed in the small Cys-SO^- peaks at 914/907 cm^{-1} (Figure 4 B, blue line). These peaks disappeared, and new peaks appeared at 890/883 cm^{-1} (Figure 4 B, red line). Although these signals are extremely small compared with other major peaks, the intensities are significantly larger than the noise level (Figure 4 B, dotted blue line). The 24 cm^{-1} downshift is comparable to the predicted ^{18}O downshift of 31 cm^{-1} in an isolated SO^- vibration.[9] This downshift of the SO^- vibration following the NHase reaction in $H_2{}^{18}O$ indicates that the oxygen atom of the Cys-SO^- group is replaced with ^{18}O from water; hence, the O atom of αCys114-SO^- is exchanged with the solvent water during the *Re*NHase nitrile hydration reaction.

A remaining issue involves the regeneration of sulfenic acid. The mechanism proposed by Hopmann, in which the thiolato ligand functions as a nucleophile to attack the S atom of the cyclic intermediate to form a disulfide bond between αCys109 and αCys114,[21] is unlikely because the distance between the S atoms of αCys109 and αCys114 remains nearly unaltered throughout the time-resolved X-ray crystallography analysis (Supporting Information, Figure S3), despite that βArg56 is not essential for the disulfide bond formation. Alternatively, the water molecule forms hydrogen bonds with the guanidinium groups of βArg56 (or the ε-amino group of βLys56 in the βR56K mutant) and βArg141 and with the two main chain amide O atoms of αThr163 and αAla164 (Supporting Information, Figure S1, wat1635 in the wild-type and wat132 in the βR56K mutant). We note that the water molecule was not involved in the theoretical analysis for the disulfide bond intermediate mechanism. The water molecule is the closest solvent molecule to the S atom of αCys114 and forms hydrogen bonds with the O atom of αCys114-SO^- in both wild-type and βR56K mutant *Re*NHases.

Therefore, we propose the following catalytic mechanism (Figure 5). First, the substrate replaces the water ligand to coordinate the metal (Figure 5, A). Second, the O atom of αCys114-SO^- attacks the C atom of the substrate CN group to form the cyclic reaction intermediate (Figure 5, B). The guanidinium group of βArg56 is likely to activate both the water molecule mentioned above and the O atom of the cyclic intermediate. In fact, over the course of the 700 min reaction, the water molecule (wat132) moves slightly toward the Nε atom of βLys56 in the βR56K mutant *Re*NHase (Supporting Information, Figure S4). Third, following the formation of the cyclic reaction intermediate, the N atom of the cyclic

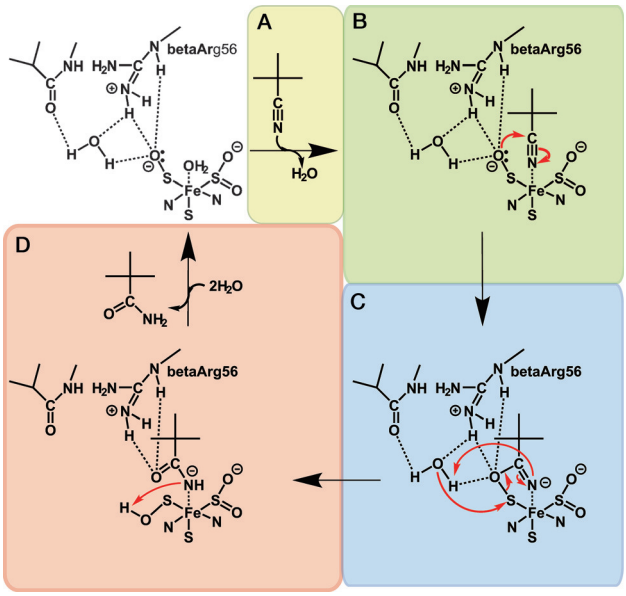

Figure 5. Proposed catalytic mechanism of NHase. The steps (A)–(D) are described in the text.

intermediate extracts a proton from the water molecule, which facilitates nucleophilic attack of the water O atom on the S atom of αCys114 and subsequent reactions (Figure 5, C). Finally, the H atom of the regenerated -SOH group is transferred to the N atom of the intermediate; and the product was released and a water molecule is coordinated to be the resting state (Figure 5, D). The decrease in the k_{cat} value of the βR56 K mutant would be ascribed to difference in the pK_a values between arginine (pK_a 12.5) and lysine (pK_a 10.5).

In conclusion, we propose the first NHase reaction mechanism in which αCys114-SO^- functions as a catalytic nucleophile and the O atom of the SO^- group is exchangeable based on the high-resolution crystal structures of the reaction intermediates of the NHase-substrate complex. This is the novel biological function of the cysteinesulfenic acid modification in biological systems. Although the hydrogen bonding networks surrounding the catalytic center and the protonation state of αCys114-SO^- should be confirmed by future studies using neutron crystallography, we have now established an outline of the NHase catalytic mechanism.

Acknowledgements

We would like to thank Prof. E. I. Solomon and Dr. K. E. Light for valuable discussion and comments. We also thank the beamline assistants at the Photon Factory for data collection at beamlines BL-5A and BL-1A. This work was supported in part by a Grant-in-Aid for Scientific Research from the Scientific Research (B) KAKENHI 21350089 (to M.O.) and (B) KAKENHI 24350082 (to M.O.). This work was performed with the approval of the Photon Factory Advisory Committee (approval nos. 2008G640 and 2011G645).

Keywords: cysteinesulfenic acid · nitrile hydratase · reaction intermediates · reaction mechanisms · time-resolved X-ray crystallography

How to cite: *Angew. Chem. Int. Ed.* **2015**, *54*, 10763 – 10767
Angew. Chem. **2015**, *127*, 10913 – 10917

[1] Y. Asano, Y. Tani, H. Yamada, *Agric. Biol. Chem.* **1980**, *44*, 2251 – 2252.
[2] a) S. Prasad, T. C. Bhalla, *Biotechnol. Adv.* **2010**, *28*, 725 – 741; b) V. G. Debabov, A. S. Yanenko, *Rev. J. Chem.* **2011**, *1*, 385 – 402.
[3] T. Li, J. Liu, R. Bai, D.-G. Ohandja, F.-S. Wong, *Water Res.* **2007**, *41*, 3465 – 3473.
[4] a) S. Nagashima, M. Nakasako, N. Dohmae, M. Tsujimura, K. Takio, M. Odaka, M. Yohda, N. Kamiya, I. Endo, *Nat. Struct. Biol.* **1998**, *5*, 347 – 351; b) A. Miyanaga, S. Fushinobu, K. Ito, T. Wakagi, *Biochem. Biophys. Res. Commun.* **2001**, *288*, 1169 – 1174; c) J. A. Kovacs, *Chem. Rev.* **2004**, *104*, 825 – 848; d) T. Yano, T. Ozawa, H. Masuda, *Chem. Lett.* **2008**, *37*, 672 – 677.
[5] T. J. Jönsson, A. W. Tsang, W. T. Lowther, C. M. Furdui, *J. Biol. Chem.* **2008**, *283*, 22890 – 22894.
[6] A. Volbeda, L. Martin, C. Cavazza, M. Matho, B. W. Faber, W. Roseboom, S. P. Albracht, E. Garcin, M. Rousset, J. C. Fontecilla-Camps, *J. Biol. Inorg. Chem.* **2005**, *10*, 239 – 249.
[7] L. B. Poole, P. A. Karplus, A. Claiborne, *Annu. Rev. Pharmacol. Toxicol.* **2004**, *44*, 325 – 347.
[8] a) C. E. Paulsen, K. S. Carroll, *Chem. Rev.* **2013**, *113*, 4633 – 4679; b) C. Jacob, E. Battaglia, T. Burkholz, D. Peng, D. Bagrel, M. Montenarh, *Chem. Res. Toxicol.* **2012**, *25*, 588 – 604.
[9] T. Noguchi, M. Nojiri, K. Takei, M. Odaka, N. Kamiya, *Biochemistry* **2003**, *42*, 11642 – 11650.
[10] K. E. Light, Y. Yamanaka, M. Odaka, E. I. Solomon, manuscript in preparation.
[11] T. Arakawa, Y. Kawano, S. Kataoka, Y. Katayama, N. Kamiya, M. Yohda, M. Odaka, *J. Mol. Biol.* **2007**, *366*, 1497 – 1509.
[12] a) T. Murakami, M. Nojiri, H. Nakayama, M. Odaka, M. Yohda, N. Dohmae, K. Takio, T. Nagamune, I. Endo, *Protein Sci.* **2000**, *9*, 1024 – 1030; b) M. Tsujimura, M. Odaka, H. Nakayama, N. Dohmae, H. Koshino, T. Asami, M. Hoshino, K. Takio, S. Yoshida, M. Maeda, I. Endo, *J. Am. Chem. Soc.* **2003**, *125*, 11532 – 11538.
[13] T. Arakawa, Y. Kawano, Y. Katayama, H. Nakayama, N. Dohmae, M. Yohda, M. Odaka, *J. Am. Chem. Soc.* **2009**, *131*, 14838 – 14843.
[14] a) W. Huang, J. Jia, J. Cummings, M. Nelson, G. Schneider, Y. Lindqvist, *Structure* **1997**, *5*, 691 – 699; b) M. Kobayashi, S. Shimizu, *Nat. Biotechnol.* **1998**, *16*, 733 – 736.
[15] a) L. Heinrich, A. Mary-Verla, Y. Li, J. Vassermann, J. C. Chottard, *Eur. J. Inorg. Chem.* **2001**, 2203 – 2206; b) R. D. Swartz, M. K. Coggins, W. Kaminsky, J. A. Kovacs, *J. Am. Chem. Soc.* **2011**, *133*, 3954 – 3963.
[16] a) S. Mitra, R. C. Holz, *J. Biol. Chem.* **2007**, *282*, 7397 – 7404; b) S. Rao, R. C. Holz, *Biochemistry* **2008**, *47*, 12057 – 12064.
[17] K. Hashimoto, H. Suzuki, K. Taniguchi, T. Noguchi, M. Yohda, M. Odaka, *J. Biol. Chem.* **2008**, *283*, 36617 – 36623.
[18] N. Gumataotao, M. L. Kuhn, N. Hajnas, R. C. Holz, *J. Biol. Chem.* **2013**, *288*, 15532 – 15536.
[19] S. Martinez, R. Wu, R. Sanishvili, D. L. Liu, R. C. Holz, *J. Am. Chem. Soc.* **2014**, *136*, 1186 – 1189.
[20] K. H. Hopmann, *Inorg. Chem.* **2014**, *53*, 2760 – 2762.
[21] C. T. Liu, S. J. Benkovic, *J. Am. Chem. Soc.* **2013**, *135*, 14544 – 14547.
[22] S. R. Piersma, M. Nojiri, M. Tsujimura, T. Noguchi, M. Odaka, M. Yohda, Y. Inoue, I. Endo, *J. Inorg. Biochem.* **2000**, *80*, 283 – 288.
[23] M. Odaka, K. Fujii, M. Hoshino, T. Noguchi, M. Tsujimura, S. Nagashima, M. Yohda, T. Nagamune, Y. Inoue, I. Endo, *J. Am. Chem. Soc.* **1997**, *119*, 3785 – 3791.
[24] T. Noguchi, J. Honda, T. Nagamune, H. Sasabe, Y. Inoue, I. Endo, *FEBS Lett.* **1995**, *358*, 9 – 12.

Received: March 24, 2015
Revised: May 26, 2015
Published online: August 14, 2015

